remote sensing

*Article*

# Planning for Sustainable Cities in Africa: Experiences, Challenges and Prospects of Monitoring Geospatial Indicators

**Shrijwal Adhikari [1,*], Preeti Koirala [2,3], Amit Ghosh [1] and Matieu Henry [1]**

1 Land and Water Division, Food and Agriculture Organization of the United Nations (FAO), 00153 Rome, Italy; amit.ghosh@fao.org (A.G.); matieu.henry@fao.org (M.H.)
2 United Nations University Institute for Environment and Human Security (UNU-EHS), D-53113 Bonn, Germany; koirala@ehs.unu.edu
3 Munich Climate Insurance Initiative (MCII), D-53113 Bonn, Germany
* Correspondence: shrijwal.adhikari@fao.org

**Abstract:** The African continent is receiving unprecedented pressure from population growth, urbanisation, decreased agricultural productivity and changing climate. However, the continent lacks technological advancement. Therefore, there is a need to apply global data and open geospatial tools for analysis to prevent, stop and comprehend the trend and effects of land degradation, food insecurity and the unsustainability of cities. The study takes three representative indicators (climate risk, land degradation and land consumption) from FAO's four strategic *better's* to demonstrate the feasibility and applicability of global datasets to support decision makers. Three representative cities in Africa are selected for the study—Houet, Burkina Faso (West Africa); Kisumu, Kenya (East Africa); and Analamanga, Madagascar (South East Africa). The study found that eight Fokontany of the Analamanga region were at high risk from climate change; at the ward level, a maximum of 54.2% of the total degraded land area in Kisumu; and maximum land-consumption rate of 1.5 was found in Houet at the department level. The results of this study can be a basis for policymakers in planning an inclusive climate-adaptation measure and sustainable land-use frameworks and policies.

**Keywords:** geospatial; sustainability of cities; land cover; global tools; open data; land degradation; land consumption



**Citation:** Adhikari, S.; Koirala, P.; Ghosh, A.; Henry, M. Planning for Sustainable Cities in Africa: Experiences, Challenges and Prospects of Monitoring Geospatial Indicators. *Remote Sens.* **2022**, *14*, 2821. https://doi.org/10.3390/rs14122821

Academic Editors: Alexandru-Ionuţ Petrişor, Dailiang Peng and Roxana Bojariu

Received: 19 April 2022
Accepted: 9 June 2022
Published: 12 June 2022



## 1. Introduction

The total population of Africa is increasing rapidly, with the total population almost doubling by 2050, and two-thirds of the population growth is projected to be absorbed in urban areas [1]. The annual population growth rate from 2010 to 2015 was 1.3% [2], with that of the world at 1.018% in 2020 [3]. Furthermore, the urban population in Africa has rapidly grown from 27% in 1950 to 40% in 2015 and is expected to reach 60% by 2050 [4]. FAOSTAT projects the total urban population to surpass the rural population between 2035 to 2040 (Figure 1) [5].

The increase in population in Africa has led to increased competition for food and natural resources. Although evidence of larger yield through limited investments exists [6,7], the reduction in crop yield and food insecurity is looming over the region as crop yield has stagnated since the 70s. For example, 153 million people over fifteen years of age suffered from severe food insecurity in sub-Saharan Africa in 2014/15 [8]. The region also has the lowest per capita income, with sub-Saharan Africa reporting one-third of the average per capita income (PCI) of the world in 2014. The leading cause of food insecurity is associated with limited investment in agriculture, disasters with severe droughts and floods leading to loss of cropland and agricultural areas, insufficient pastures to graze and feed livestock, and traditional and unmechanised farming systems [8].

The impacts of climate change have a greater impact on the African continent, and the continent's low and fragile economy further exacerbates the impacts. According to the

IPCC AR6 report, agricultural productivity has been greatly impacted by climate extremes and the sector has faced higher economic losses. In addition, a decline in vegetation and enhanced desertification due to climate change is expected. For example, in the Sahara and Sahel, the rainfall is projected to drop, leading to soil degradation and an increase in the frequency of dust storms. As a result, agricultural production is severely affected, which is already reeling under poor irrigation and traditional farming methods [9,10]. This has put tremendous pressure on 250 million smallholding farmers who own crop farms of less than five hectares [11].

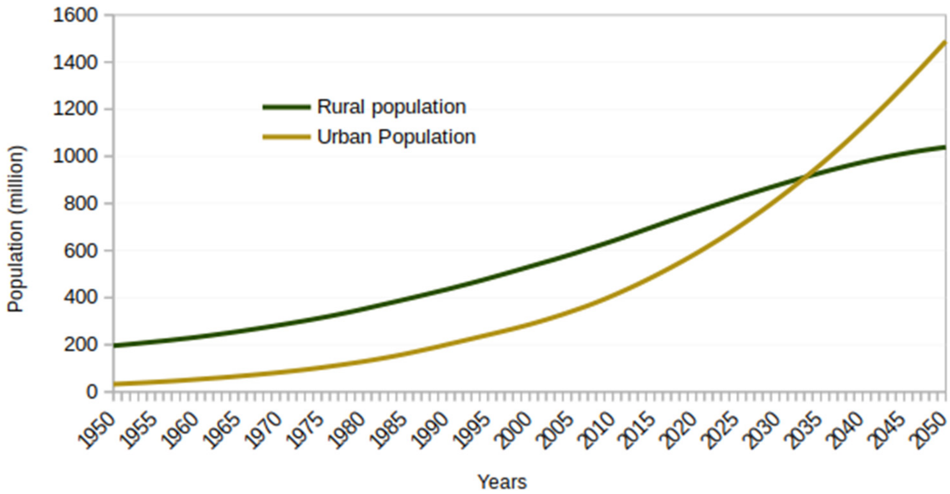


**Figure 1.** Urban and rural population growth in Africa [5].

Despite being one of the most vulnerable regions globally, climate change studies in East, West and Central Africa are limited. About two-thirds of the land resources in Africa have degraded to a certain degree [12]. Human activities have led land-use and land-cover changes, resulting in land degradation [13], and climate change has further increased the risk [12]. Agriculture and income are the two driving factors behind environmental degradation [14]. While increasing population leads to environmental damages, a higher income level lowers negative impacts on the environment due to agricultural practices. Agriculture is crucial for the economy of many of the countries in the African subcontinent. Lack of proper land-management practices, natural-resource management and agricultural practices, particularly among farmers with poor economic backgrounds, has further contributed to the region's environmental and land-degradation problems [12]. The region's population is increasing rapidly, which leads to the expansion of agricultural activities to meet the needs of the growing population [14]. Varying climatic conditions, conflict, war and deforestation are also the driving factors for land degradation in Africa [12,14,15].

Therefore, there is an established need to measure the indicators to better plan for sustainable cities in the wake of climate change, population growth and pressure, and an increase in food demand with limited land resources and productivity. FAO's four pillars [16] based on the *four betters* aim to transform the agri-food system and make it more efficient, inclusive, resilient and sustainable. First, better production aims at efficient and inclusive agriculture and food supply chains at local, regional and global levels to ensure sustainable consumption and production in the wake of climate change. Second, better nutrition targets end food hunger, attain food security, better nutrition and improved access to healthy diets. Third, better environment's goal is the sustainable use of ecosystems and resources for agri-food systems and addressing climate change. Lastly, better life focuses on reducing inequalities and encouraging inclusive economic growth.

The main aim of this study is to select three representative indicators—climate risk assessment, land degradation and land-consumption rate—and demonstrate the applicability and feasibility of the selected indicators to better plan for sustainability and greening of cities using global data and tools. First, the climate risk assessment is carried through the change in parameter of length of the growing period. Second, land degradation (SDG 15.3.1) is assessed as a function of change in land cover, land productivity and soil organic carbon. Third, the land-consumption rate (SDG 11.3.1) is derived as a function of changes in urban area and population. The study can be carried out with minimal local data. These indicators are chosen in the framework of FAO's *four betters* and address the goals of the *four betters*. The selected indicators consider climate change, investigate the impacts and pressure of the rapidly growing population on the available resources, increasing food demand and land degradation. The objective of this study is to (a) assess climate risk for the future projected scenarios using the length of the growing period and population data; (b) measure degraded land; and (c) measure the land-consumption rate to demonstrate the applicability of global and open data and tools for the measure of indicators in support to greening and sustainability of cities.

## 2. Materials and Methods

### 2.1. Study Area

For this research, three cities in Africa were selected for each indicator. Houet in Burkina Faso was selected to assess the land-consumption rate, Kisumu in Kenya was selected for land degradation, and Analamanga in Madagascar was selected for climate risk assessment. The selected study areas are from the eastern, north-western and south-eastern regions of Africa. The three study areas' economies are highly dependent on agriculture and face the challenge of a rapidly growing population, food insecurity, pressure on land, and the looming threat of climate change. Therefore, the three areas, as shown in Figure 2, located in different regions of Africa, are a sample study area selected as a representative for the entire continent of Africa.

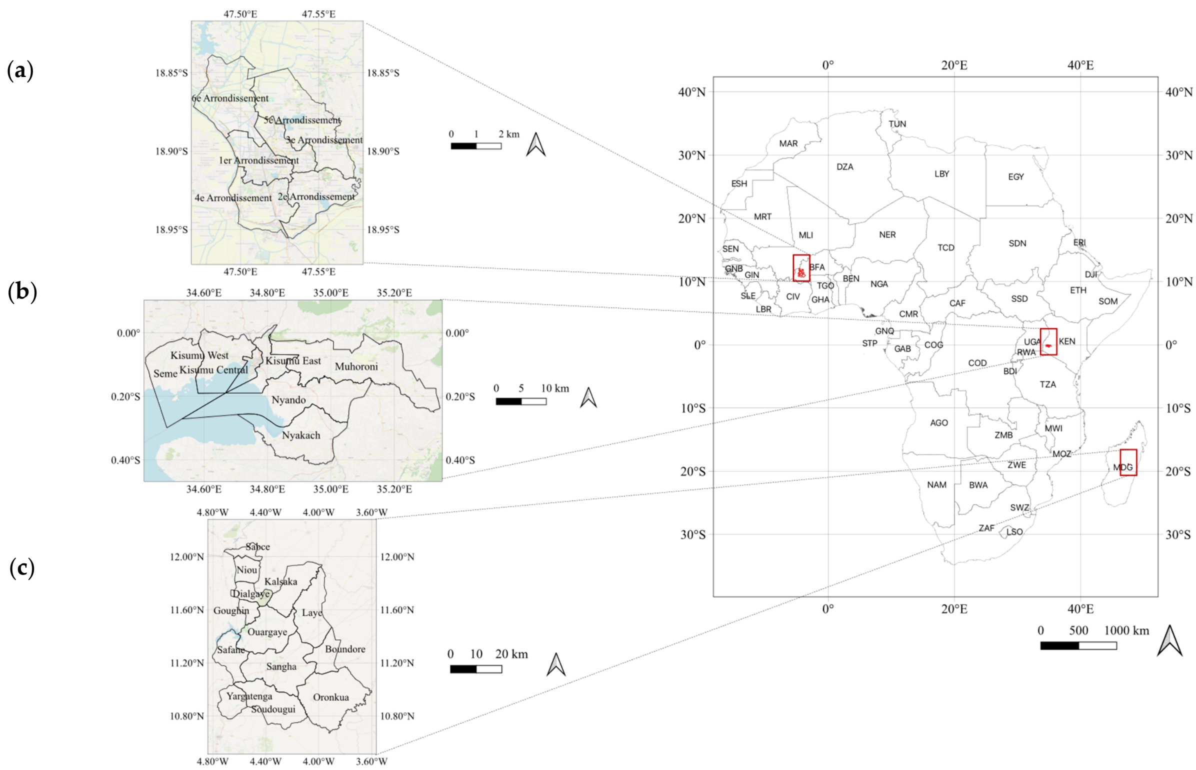


**Figure 2.** Location map of the study area: (**a**) Houet (Burkina Faso), (**b**) Kisumu (Kenya), (**c**) Analamanga (Madagascar) in Africa.

#### 2.1.1. Analamanga, Madagascar

Madagascar is an island nation on the south-eastern coast of Africa. With an area of approximately 590,000 sq.km, it is the fourth-largest island globally. About 61.1% of the country's population lives in rural areas. The island nation has a wide range of vegetation habitats: humid tropical forest to arid semi-desert, which receives an average annual rainfall of 3500 mm and 350 mm, respectively. Agriculture is the backbone of the country's economy. The native forests in the country are converted for agricultural purposes; after the soil quality degrades, the land is abandoned [17–19]. The capital Antananarivo lies in the Analamanga region and is the largest city, covering an area of 86.4 sq.km and a population of roughly 1.3 million, which is 30% of the urban population. The tropical mountain city is situated in the central highland region of Madagascar at an altitude of 1280 m above sea level. Human settlements are centred on the hills, whereas the lowlands, plains and valleys are used for agricultural purposes. The agricultural area accounts for 43% of the total area of Antananarivo, with rice fields being the most significant land-use type. However, rapid urbanisation has led to encroachment of traditional rice plains, resulting in soil- and water-resource degradation. Furthermore, as the city is situated on a hill, the scope of expanding the metropolitan area is limited [19–21]. The island nation is exposed to climate risks and vulnerable to climate impacts. Loss of forest habitat has resulted in making the country more vulnerable to climate change. The region experienced continuous increase in temperature and variable rainfall patterns consequently affecting the hydrological cycle. The country was hit with cyclones. In 2004, cyclones Elita and Gafilo resulted in 2.3% GDP loss, whereas in 2006 cyclone Boloetse resulted in 0.7% GDP loss. Additionally, drought across the country has affected maize crop production. It is projected that climate change will result in frequent droughts, cyclones and a rise in sea levels [18,22,23].

#### 2.1.2. Kisumu, Kenya

Kenya spans along the equator in the Eastern part of Africa. With an area of 582,646 sq.km, 98.1% is landmass, whereas the remainder, 1.9%, is water bodies. The country's climate is categorised into seven agroclimatic zones based on the varying climatic conditions [24,25]. The study area, Kisumu, is situated on Lake Victoria and lies in the western part of Kenya. It is the third-largest city in Kenya and the capital of Nyanza province [26]. As the city is situated in the equatorial region, it experiences a tropical rainforest climate. Hence, the region experiences a warm to hot and wet climate with a mean temperature of 22.9 °C and mean annual rainfall of 1490 mm. The port city covers an area of 546 sq.km with a population of about 335,000 [27]. Western Kenya is a predominantly agroeconomic region, and with a growing population and high population density of 130–150 people/sq.km, the land is experiencing increasing pressure. The majority of the population, accounting for up to 90%, rely heavily on agriculture as a source of their income. An average farm measures about 0.6 ha [28,29]. Additionally, 53% of the population lives under the poverty line. Erratic rainfall patterns, droughts and floods have adversely affected food security for the people. The city's location has economic and political importance within the East African region [28,30,31]. Added to that, land degradation is a major problem in the African continent. Annually, soil erosion has resulted approximately 2–40% decrease in agricultural productivity. The scenario is similar in Kenya, affecting millions of people. The extent and severity of land degradation is increasing with 20% of cultivated areas, 30% of forests and 10% of grassland degraded [32]. Human activities have resulted in 12% of degraded land, where 27% of the population resides. The contributing factors behind land degradation are deforestation and bad agricultural practices. Furthermore, county governments, and in particular the farmers in Kenya, are more concerned about soil erosion [32,33].

#### 2.1.3. Houet, Burkina Faso

In the western part of Africa lies the landlocked country of Burkina Faso. With an area of approximately 274,000 sq.km it has a population of about 19 million. The population in the country is rapidly increasing, with an annual population growth rate of 3% in 2016. Burkina Faso has a short rainy season from June to October and an extended dry season from November to May. The average annual rainfall is 1100 mm in the south and 300 mm in the north. Likewise, the mean monthly temperature varies throughout the country. The northern part of the country, situated in the Sahel zone or the Sahelian Acacia Savanna, has a mean monthly temperature between 23 °C and 34 °C. The southern part located in the Sudanian Savanna experiences temperature between 25 °C and 31 °C. Burkina Faso's economy depends on agriculture, livestock and forestry sectors [34–36]. The province of Houet lies in the western part of Burkina Faso and has an area of 11,582 sq.km. It is located in the South Sudanian Climatic Zone and experiences an alternating wet and dry season, with the average annual rainfall in Houet being 1200 mm. The province is a significant region for rice cultivation [37]. Globally, 10–15% of land-use change is attributed to agriculture and urban expansion, and 6% to pastural land. Burkina Faso has also seen a drastic land-cover change due to external forces such as rapid population growth, internal migration and poverty. For example, a decrease in rainfall and availability of arable land in the north and central Burkina Faso led to internal migration of farmers to the south [38,39].

### *2.2. Methodology*

The present study relies on the three case studies: (a) measure of the risk due to change in climate in Analamanga (Madagascar), (b) the measure of land-consumption rate (SDG 11.3.1) in Houet, Burkina Faso, and (c) the measure of degraded area (SDG 15.3.1) in Kisumu, Kenya. The overall methodology consists of selecting an area of interest, preparing the indicators of measure and aggregating the indicators at the subcounty (Kisumu), department (Houet) or Fokontany level (Analamanga).

#### 2.2.1. Case Study 1: Measure of Risk Associated with Climate Change in the Analamanga Region of Madagascar

i. Description of the terminology and input data

The length of the growing period (LGP) is defined as "the agro-climatic potential productivity of land in number of days in a year when temperature regime and moisture supply are conducive to the crop growth and development" [40]. LGP is associated with the land productivity and agroclimatic potential of land. It is the result of the combined effect of suitable temperature, water stress in terms of soil moisture and humidity responsible for the growth and development of crops. Since LGP is a representative parameter of the combined climatic necessities for crop development, it is used as an indicator for measuring the effect of changing climate. The administrative boundary is obtained from GADM at Fokontany (admin level 4), LGP data from the GAEZ platform [41], and population data from Worldpop for the year 2020 [42] are used (Table 1).

**Table 1.** Input data for assessing the risk of changing climate in the Analamanga region of Madagascar.

| Input Data | Source |
|---|---|
| Administrative boundary level 4 (Fokontany) | GADM |
| Length of growing period (LGP) | GAEZ data |
| Population data | Worldpop |

ii. Methods

The workflow to measure future climate risks is presented in Figure 3. The LGP data for the historical period (1981–2010) were obtained through the CRUT32 model and future scenarios (under RCP 2.6, 4.5 and 8.5 for 2041–2070) through the ENSEMBLE climate model from the GAEZ data. The population data (per pixel) of Madagascar for 2020 were acquired from Worldpop. Next, the population data and LGP data were clipped to the Analamanga region. Average LGP days during the historical and projected future periods were computed using zonal statistics from QGIS desktop software. Then, the change in LGP days in future scenarios was calculated as a difference from the historical period (Table 2). The change in LGP was normalised for RCP 2.6, RCP 4.5 and RCP 8.5 scenarios. Next, the total population at each Fokontany was computed and normalised. Finally, the risk of changing climate was calculated as the function of normalised LGP change (a proxy for hazard) and normalised population (a proxy for exposure) using Equation (1). Due to unavailability of global and observation data on the hazard impact (vulnerability) which propagates into the livelihood of the society, risk was calculated as a function of hazard and exposure [43]. Empirically (Equation (1)):

$$\text{Risk} = \text{Hazard (LGP change)} \times \text{Exposure (population)} \tag{1}$$

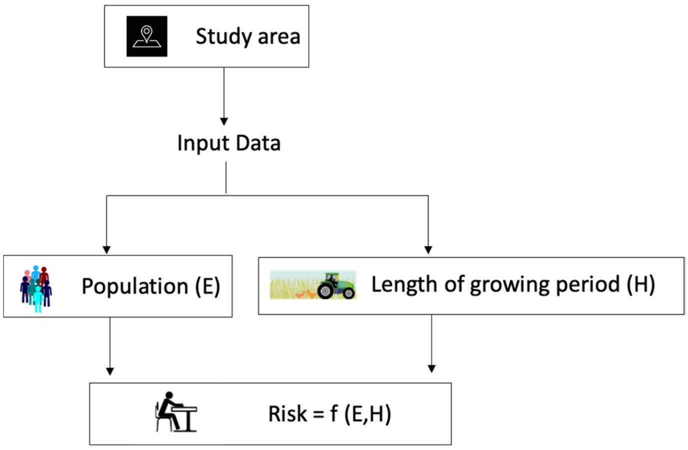


**Figure 3.** Workflow to measure future climate risk through the change in length of growing period (LGP) and population.

**Table 2.** Summary of population and change in length of the growing period in the Analamanga region, Madagascar.

| Population Class (nb) | Fokontany (nb) | Length of Growing Period (LGP) Change | | | | | |
|---|---|---|---|---|---|---|---|
| | | Change at RCP 2.6 (Days) | Fokontany (nb) | Change at RCP 4.5 (Days) | Fokontany (nb) | Change at RCP 8.5 (Days) | Fokontany (nb) |
| <10,000 | 168 | ≤5 | 23 | ≤5 | 14 | ≤20 | 18 |
| 10,000–50,000 | 23 | 5–10 | 3 | 5–10 | 11 | 20–25 | 113 |
| >50,000 | 1 | 10–15 | 166 | 10–15 | 167 | >25 | 61 |
| Total | 192 | | 192 | | 192 | | 192 |

2.2.2. Case Study 2: Measure of Land Degradation (SDG 15.3.1) in Kisumu, Kenya

i. Description of the terminology and input data

SDG 15.3.1 measures the proportion of degraded land over total land area. Land degradation is defined as “the reduction or loss of the biological or economic productivity and complexity of rain fed cropland, or range, pasture, forest, and woodlands, resulting from a combination of pressures, including land use and management practices” [44]. The indicator is measured from three sub-indicators, viz. (a) land-cover change, (b) land-productivity change and (c) soil organic carbon (SOC) change. The input parameters are summerised in Table 3. The land cover for the years 2016 and 2020 was generated using a subset of Africover legend [45] for Kenya. Change in land productivity was measured from the annual series of NDVI from Landsat 8, and baseline soil organic carbon data were obtained from Soil Grids [46]. Further, to assess the available land for tree plantation and hedgerow plantation around parcels in the degraded area, image segmentation of NICFI planet data was carried out to delineate the parcels.

**Table 3.** Input data for measuring degraded land (SDG 15.3.1) and delineating parcels for hedgerow and tree plantations.

| Input Data | Source |
|---|---|
| Administrative boundary level 2 (county) | UNOCHA-HDX |
| Land cover for 2016 and 2020 | Generated from Sentinel 1 and 2 imageries |
| Satellite imagery | Sentinel 1 and 2, Landsat 8 and NICFI planet |
| Productivity index | NDVI |

ii. Methods

a. Preparation of study area and generating the land-cover map

Figure 4 summarises the workflow to delineate the area for tree plantation from degraded area. The administrative boundary at the subcounty level of Kisumu was obtained from UNOCHA-HDX. Land-cover legends for Kisumu were prepared from the subsets of Africover land cover of Kenya (2000), as shown in Figure 5. A total of 2600 training points, 200 each for thirteen land-cover classes, were collected manually using the visual interpretation of very-high-resolution satellite imagery (e.g., Bing and Google) and spectral indices of NDVI for the year 2020. After collecting training points, the satellite imageries from Sentinel 1 and 2 were mosaicked for 2016 and 2020. To preserve the phenology of vegetation, imageries were prepared for summer, spring, autumn and winter seasons. A random-forest model was trained in Google Earth Engine using training points and applied over 2020 imagery for classification. 70% of training data were used for actual training, and the remaining 30% were used for in-sample validation. The land-cover classification for 2020 was obtained at Kappa 74% and Producer Accuracy of 77%. The model prepared with training points for the year 2020 was used for classifying the imagery from 2016.

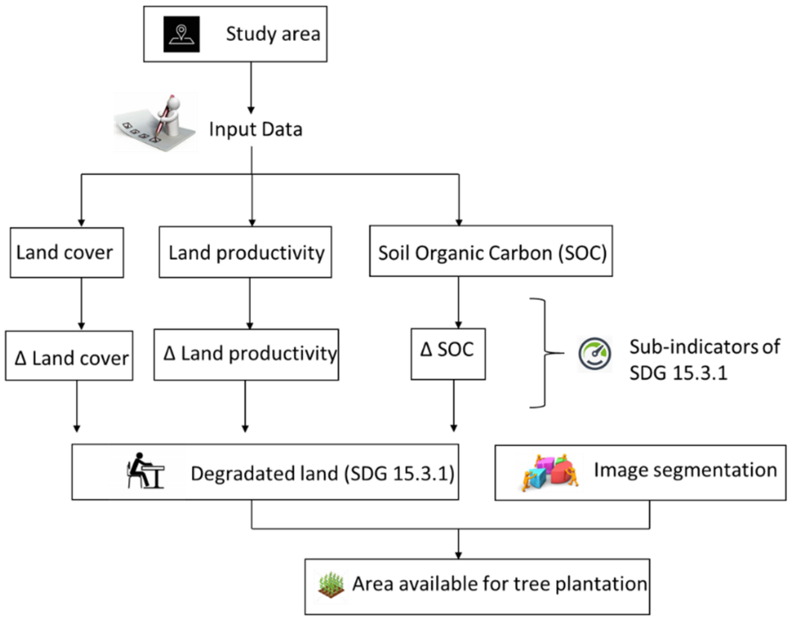


**Figure 4.** Workflow to delineate areas for tree plantation from degraded areas (SDG 15.3.1).

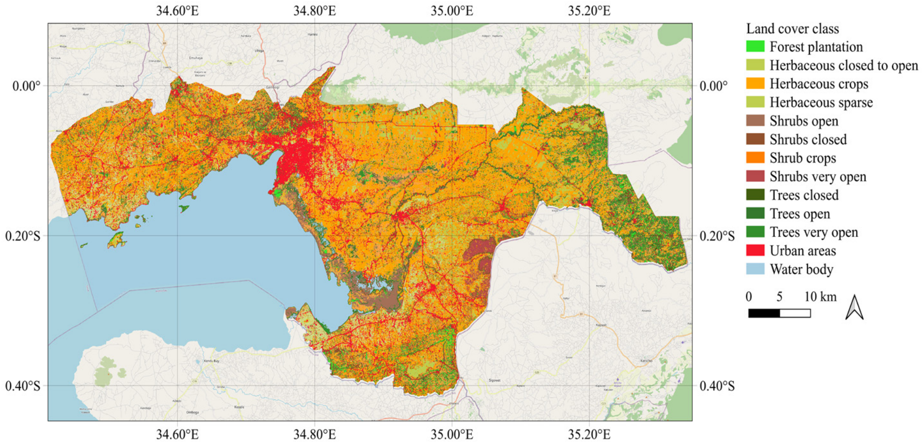


**Figure 5.** 2020 land-cover map of Kisumu prepared from the subsets of Africover legends of Kenya (2000).

b. Preparation of land-degradation (SDG 15.3.1) sub-indicators

Land-cover change, land-productivity change and SOC change are the three sub-indicators for SDG 15.3.1. The methods for measuring these sub-indicators are described in the following subsections.

1. Preparation of a land-cover change matrix and measurement of land-cover change

The thirteen land-cover classes were reclassified to align with six IPCC land-cover classes as shown in Table 4. Then, a transition matrix was prepared, as shown in Table 4, to define the transitions between 2016 and 2020 as either degraded, stable or improved, as defined by UNCCD. The land-cover change was defined according to the IPCC transition class.

**Table 4.** Land-cover change transition matrix for six IPCC classes. Boxes are colour-coded as improved (green), stable (blue) or degraded (orange).

| | | **Final Class** | | | | | |
|---|---|---|---|---|---|---|---|
| | IPCC class | Forest | Grassland | Cropland | Wetland | Settlement | Bare Land |
| **Original Class** | Forest | | | | | | |
| | Grassland | | | | | | |
| | Cropland | | | | | | |
| | Wetlands | | | | | | |
| | Settlement | | | | | | |
| | Bareland | | | | | | |

2. Preparation of land-productivity data and measurement of land-productivity change

Land productivity was measured through the NDVI of Landsat 8. In addition, a series of annual land productivity was prepared from 2016 to 2020, and its metrics of productivity trend, performance and state were prepared following the Good Practice Guideline v2 from the United Nations Convention to Combat Desertification (UNCCD) [47].

3. Preparation of soil organic carbon (SOC) data and Measurement of SOC change

In order to prepare the SOC baseline data, the soil grid and the change in SOC was calculated following the Good Practice Guidelines (GPG) v2 from UNCCD.

Following the measurement of SDG 15.3.1 sub-indicators, SDG 15.3.1 was calculated on a pixel-by-pixel basis using the one-out-all-out principle (1OAO) principle, meaning if any of the pixels are classified as degraded, the final measure of the pixel is degraded. For the present study, the SDG 15.3.1 module of the SEPAL platform [48] from FAO was used for the analysis.

4. Image segmentation to delineate parcels

Image segmentation and delineation of parcels were carried out in Google Earth Engine using NICFI planet data at 5 m spatial resolution. With the purpose of tree or hedgerow plantation around the boundary of parcels, the parcels were further delineated for boundaries of parcels.

5. Overlaying the degraded area with parcels to prioritise the plantation areas

Finally, the parcels were overlayed over the degraded areas and classified as high-priority areas for plantation. Other classes of stable and improving land overlaid with parcels were classified as medium- and low-priority plantation areas, respectively, as shown in Figure 6.

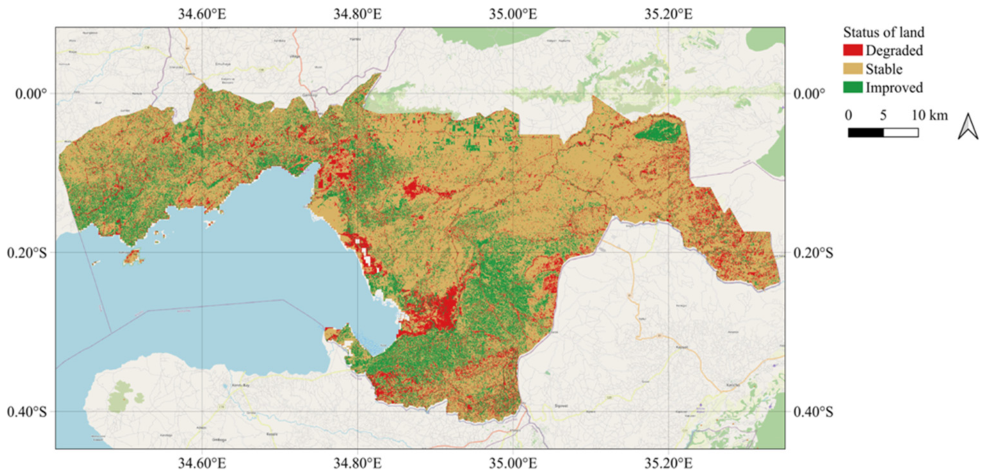


**Figure 6.** The extent of land status (degraded, stable or improved) (SDG 15.3.1) between 2016 and 2020 in Kisumu, Kenya.

2.2.3. Case Study 3: Measure of Land-Consumption Rate (SDG 11.3.1) in Houet, Burkina Faso

i. Description of the terminology and input data

SDG 11.3.1 is the measure of the land-consumption rate. The land-consumption rate is defined as "the ratio of land consumption rate to the population growth rate" [44]. The indicator measures the extent of the urban area built to the population change. Input data listed in Table 5 were acquired from various sources to measure the indicator. The administrative boundary at the department level (admin level 3) was acquired from GADM, and the land cover for Houet was generated using subsets of Observatory for Sahara and Sahel (OSS) Legends for Burkina Faso (2016) for 2016 and 2020 and population data were obtained from Worldpop for 2016 and 2020.

**Table 5.** Input data to measure land-consumption rate (SDG 11.3.1).

| Input Data | Source |
| --- | --- |
| Administrative boundary level 3 (department) | GADM |
| Land cover for 2016 and 2020 | Generated using Sentinel 1 and 2 imageries |
| Population data for 2016 and 2020 | Worldpop |

ii. Methods

a. Preparation of study area and generating the land-cover map

The summary of the methodological approach in deriving the land-consumption rate is shown in Figure 7. The administrative boundary at the department level of Houet province was obtained from GADM. Land-cover legends for Houet were prepared from the subsets of the OSS land cover of Burkina Faso (2016). A total of 2400 training points, 200 each for the twelve land-cover classes, were collected manually using the visual interpretation of very-high-resolution satellite imagery (e.g., Bing and Google) and spectral indices of NDVI for the year 2020. After collecting training points, the satellite imageries were mosaicked from Sentinel 1 and 2 for the years 2020 and 2016. To preserve the phenology of vegetation, imageries are prepared for rainy and dry seasons. A random-forest model was trained in Google Earth Engine using training points and applied over 2020 imagery for classification. 70% of training data were used for actual training, and the remaining 30% for in-sample validation. The land-cover classification for 2020 was obtained at Kappa 84% and Producer Accuracy of 85%. The same model was prepared with 2020 training points and used to classify 2016 imagery. The land-use map of Houet is presented in Figure 8.

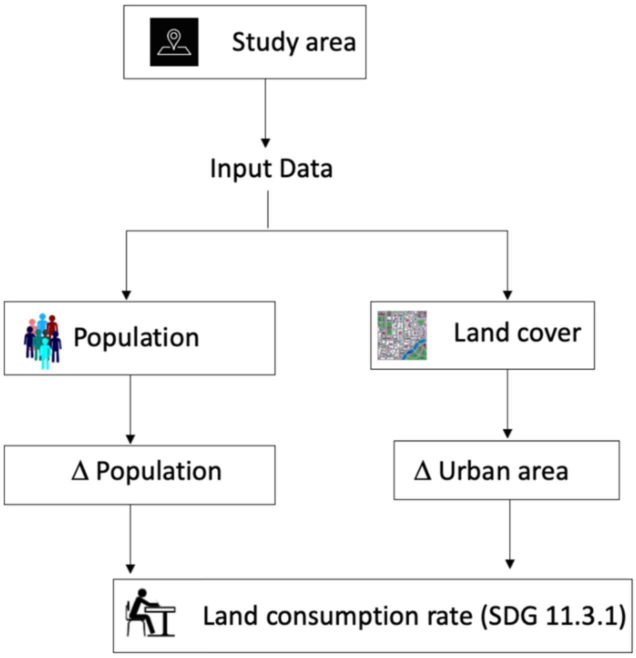


**Figure 7.** Workflow to measure land-consumption rate (SDG 11.3.1).

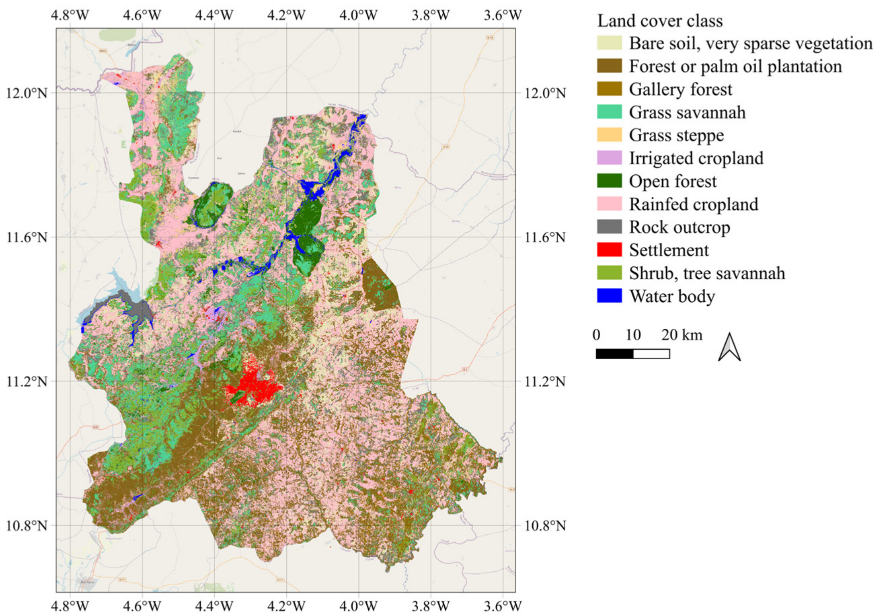


**Figure 8.** 2020 land-cover map of Houet prepared from the subsets of legends from the Observatory for Sahara and Sahel (OSS) of Burkina Faso (2016).

b. Preparation of population data

The population data for 2016 and 2020 obtained as population per pixel (100 m resolution) from Worldpop were aggregated at departments of Houet. Additionally, changes in population from 2016 to 2020 were tabulated.

c. Masking the non-urban area from land cover and preparing the change

All other land-cover classes except built-up areas were masked, and the statistics were prepared at the department level. Furthermore, the change in built-up areas from 2016 to 2020 was prepared.

d. Measurement of land-consumption rate

After changes in urban areas and an increase in population between 2016 to 2020 were calculated, the land-consumption indicator was calculated using Equation (2).

$$\text{Land consumption rate} = \frac{\Delta\ \text{built up area}}{\Delta\ \text{population}} \tag{2}$$

## 3. Results

### 3.1. Case Study 1: Climate Risk Assessment in the Analamanga Region of Madagascar

The result in Table 6 shows that 8, 95 and 89 Fokontany of the Analamanga region are at high, medium and low risk from climate change impacts on agriculture with the RCP 2.6 scenario. The number of Fokontany increased to 8, 66 and 118 at high, medium and low risk for the RCP 4.5 scenario. However, the number of Fokontany decreased to 6, 59 and 127 at high, medium and low risk for the RCP 8.5 scenario. The six Fokontany at high risk for the RCP 8.5 scenario are Soavimasoandro, Androhibe, Ambodivoanjo Ambohijatovo Fara, Analamahitsy Tanana, Amorona and Ambaravarankazo. Two additional Fokontany at high risk for the RCP 4.5 and 2.6 scenarios are Alarobia Amboniloha and Ambatobe.

**Table 6.** Number of Fokontany in Analamanga region at risk class.

| Scenario | Risk Class (Number of Fokontany) | | | Total (nb) |
|---|---|---|---|---|
| | Low | Medium | High | |
| RCP 2.6 | 89 | 95 | 8 | 192 |
| RCP 4.5 | 118 | 66 | 8 | 192 |
| RCP 8.5 | 127 | 59 | 6 | 192 |

The map of the Analamanga region with different risk classes for the three future scenarios, RCP 2.6, RCP 4.5 and RCP 8.5, is presented in Figure 9.

### 3.2. Case Study 2: Degraded Land in Kisumu County of Kenya

The land-degradation indicator (SDG 15.3.1) (Table 7), shows that land degradation ranges from 940 ha in Kisumu Central to 7684 ha in Muhorini subcounty, representing 12% to 25% of total land area, Figure 10, respectively. Muhorini, Nyakach and Nyando subcounties follow with higher values for degraded areas. Results are further disaggregated at the ward level, and it shows that Migosi (54.2%), Manyatta' B' (42.9%) and Kondele (39.8%) are the top three wards with highly degraded areas by percentage. Similarly, Miwani (6.7%), Nyang'oma (7.4%) and Ombeyi (8.9%) rank in the bottom three by percentage for degraded areas.

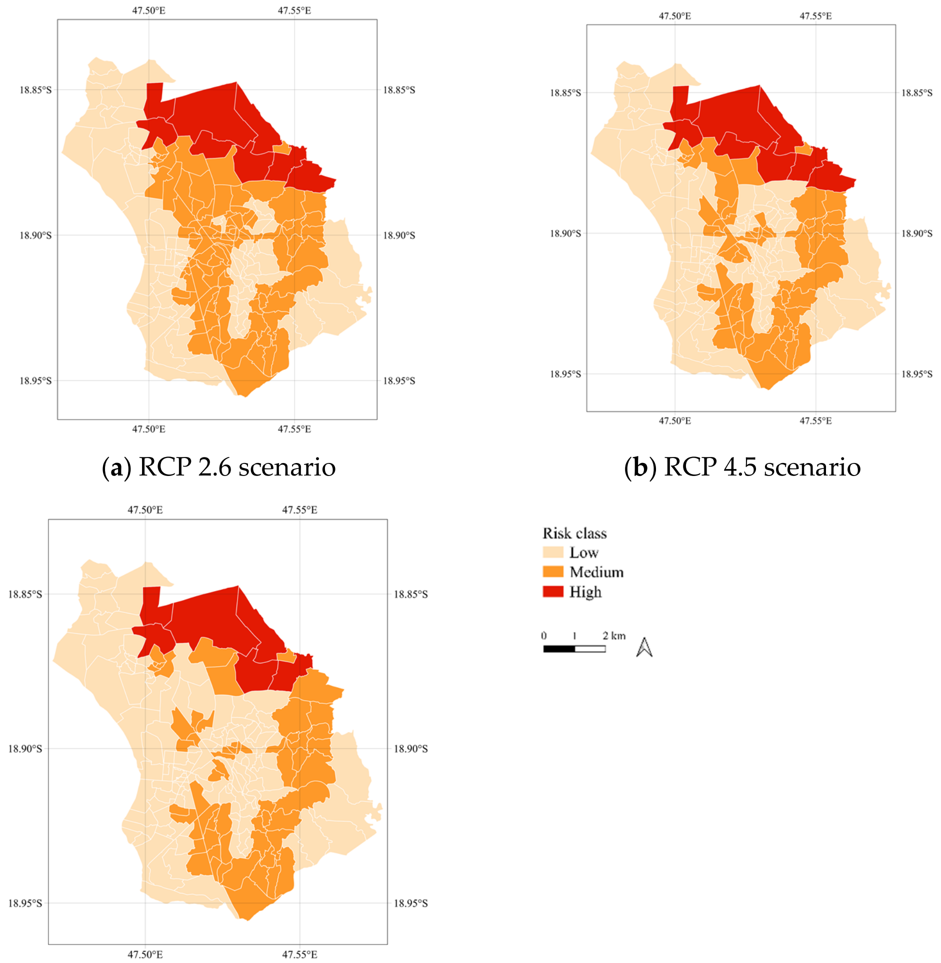


(**a**) RCP 2.6 scenario (**b**) RCP 4.5 scenario

(**c**) RCP 8.5 scenario

**Figure 9.** Risk class calculated as a function of change between historical (1981–2010) and future projected (2041–2070) period through length of growing period (LGP) and the population in Fokontany level, Analamanga region, Madagascar at RCP 2.6, 4.5 and 8.5 scenarios.

**Table 7.** The extent of land status (ha) between 2016–2020 in the Kisumu subcounty.

| Sub-County | Degraded | Stable | Improved | Total |
|---|---|---|---|---|
| Muhoroni | 7684 | 52,274 | 6406 | 66,364 |
| Nyakach | 7116 | 17,449 | 11,559 | 36,124 |
| Nyando | 4868 | 26,758 | 9354 | 40,980 |
| Kisumu West | 2814 | 13,622 | 5231 | 21,666 |
| Seme | 2773 | 16,834 | 8042 | 27,648 |
| Kisumu East | 2023 | 7878 | 3838 | 13,739 |
| Kisumu Central | 940 | 2137 | 647 | 3725 |
| Muhoroni | 7684 | 52,274 | 6406 | 66,364 |

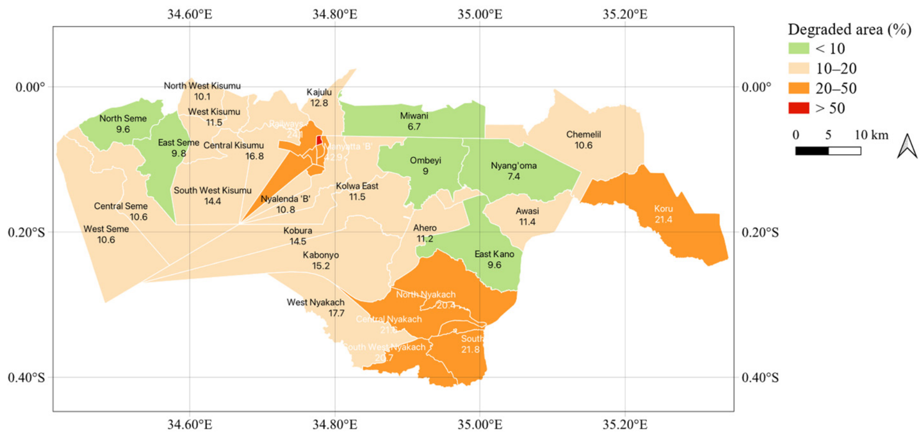


**Figure 10.** The proportion of degraded land (%) between 2016 and 2020 in Kisumu wards, Kenya.

Next, the degraded, stable and improved land are overlayed over the parcel to prioritise tree and hedgerow plantation areas as high, medium and low class, respectively (Figure 11).

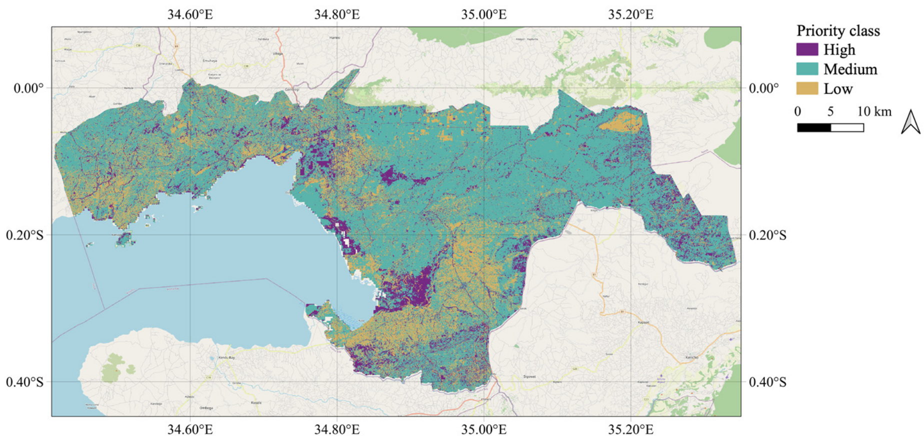


**Figure 11.** The extent of priority land available for trees and hedgerow plantation around parcels in Kisumu, Kenya.

The result in Table 8 shows that the high-priority available land ranges from 307 ha in Kisumu Central to 2703 ha in Muhoroni for tree plantation around parcels.

**Table 8.** The land availability at different priority classes for tree and hedgerow plantations in Kisumu, Kenya.

| Subcounty | Areas (ha) with Priority Class | | | |
|---|---|---|---|---|
| | **High** | **Medium** | **Low** | **Total** |
| Muhoroni | 2703 | 18,318 | 2172 | 23,193 |
| Nyakach | 2444 | 5256 | 3636 | 11,336 |
| Nyando | 1694 | 8840 | 3000 | 13,534 |
| K. West | 958 | 4376 | 1661 | 6995 |
| Seme | 926 | 5324 | 2503 | 8753 |
| K. East | 653 | 2564 | 1185 | 4403 |
| K. Central | 307 | 657 | 216 | 1180 |
| Muhoroni | 2703 | 18,318 | 2172 | 23,193 |

### 3.3. *Case Study 3: Land-Consumption Rate in Houet Province of Burkina Faso*

The land-consumption rate (SDG 11.3.1) for Houet province between 2016 and 2020 is presented in Table 9. The rate ranges from 1.1 in Bobo-Dioulasso to 1.5 in Lena. The top three departments with the highest land consumption rate are Lena (1.5), Karankasso-Vigue (1.3) and Koundougou (1.3), and the bottom three departments with lower land consumption rates are Bama (1.2), Faramana (1.1) and Bobo-Dioulasso (1.1), as presented in Figure 12.

**Table 9.** The number of departments with land-consumption rate class in Houet, Burkina Faso.

| Rate (Ratio) | Department (nb) |
|---|---|
| 1.1–1.2 | 5 |
| 1.2–1.4 | 7 |
| 1.4–1.6 | 1 |
| Total | 13 |

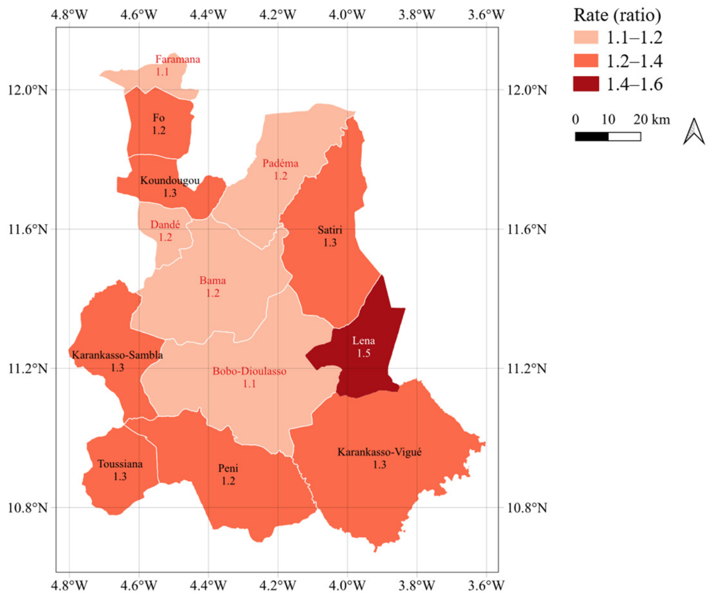


**Figure 12.** Land-consumption rate (SDG 11.3.1) between 2016 and 2020 in Houet, Burkina Faso.

## 4. Discussion

### *4.1. Case Study 1: Climate Risk Assessment in the Analamanga Region of Madagascar*

For this study, the parameter length of growing period (LGP) is selected to measure the climate risk at the projected (RCP 2.6, RCP 4.5 and RCP 8.5) scenarios from GAEZ data. The LGP data are fundamental to land productivity when temperature and moisture supply facilitate crop growth. Therefore, unlike yield, suitability area and attainable production, which are specific to crop, LGP covers a broad dimension of agricultural production relating directly to agroclimatic potential productivity in days.

The steps and the analysis are simple and easy to formulate to assess the overall risk associated with climate change in agricultural production. Based on the study findings, the cities can be prioritised for high, medium and low risk. This would aid the local authorities in developing better plans and policies for the cities against the impacts of climate change on urban and periurban agriculture. The study also demonstrates the use of global tools and data aggregated at the lower administrative level (here, Fokontany) to prioritise the areas for any planned interventions (such as climate adaptation programmes).

The analysis, however, may not be representative of the impacts in the African continent itself. The regional climate assessment varies considerably within Africa. For instance, in East Africa, the temperature is expected to rise from 0.5 degrees to 3 degrees with an increase in the precipitation and shift in intraseasonal rainfall by 2050 [49], whereas the temperature is projected to rise from 1.6 degrees to 2.9 degrees by 2050 with reduced rainfall in the extreme west of West Africa [50]. Such differences in temperature and rainfall patterns are expected to have considerable difference in the agricultural production across the continent.

### 4.2. Case Study 2: Degraded Land in Kisumu County of Kenya

The study used both global (productivity, SOC) and local data (land cover) to generate the data for measuring the degraded land in publicly available cloud performing tools (GEE and SEPAL). However, the land cover generated following the national land-cover legend is challenging, both with the availability and resolution of data. Therefore, to use the finest (10 m) resolution data for generating land cover, the assessment was carried out using 2016 and 2020 data.

Degraded land is the measure of areas that fail to serve biodiversity, ecosystem services, nutrient cycling and lower production and yield [51]. Information on degraded land is crucial to identify the hotspots and plan for actions that include the conservation, rehabilitation, restoration and sustainable management of land resources. The measure also helps address the emerging pressures on land to help avoid future land degradation, which is the first step in greening cities and making cities sustainable in terms of equitable use of resources under growing populations and changing climate. The delineation of parcels to derive available land for tree and hedgerow plantation in degraded land is an addition of ancillary data for greening and sustainability of cities through the measure of degraded land.

The present analysis is, however, limited to the assessment through satellite imagery. Deforestation in the form of timber harvesting for large-scale commercial forestry, shifting cultivation and slash-and-burn agriculture are common drivers of land degradation in Africa [15,52]. The assessment of degradation through land-cover changes such as conversion of cropland to settlement area may not be as evident as conversion of grassland to cropland through remote-sensing techniques. Further, external forces such as commercial agriculture can play a role in degradation of land, which cannot be directly observed from remote sensed imageries. In addition, the change in land-cover and land productivity in the framework of degraded land is context-specific. The conversion of land as a result of shifting cultivation and large-scale commercial forestry for timber disbalances the overall ecosystem, degrades the overall functioning of the ecosystem and ultimately degrades the land in the long run.

There is also evidence of farmland fragmentation using unmanned aerial vehicles (UAV). In the Qilu Lake watershed of China, UAVs were used to measure the forms, scenarios and drivers of farmland fragmentation and its impact on agricultural production efficiency [53]. A case study on Rwanda demonstrates that physical drivers of such fragmentation, used as a risk-management strategy, have positive impacts on the nutritional balance for food quality and food sustainability, both being the integral components of food security [51].

### 4.3. Case Study 3: Land-Consumption Rate in the Houet Province of Burkina Faso

The study used global data (population data) and local data (national land-cover legend) to derive the land-consumption rate. The latest and finer available data, with 10 m resolution, was used for 2016 and 2020. The satellite imagery was acquired from Sentinel 2 and 100 m population data from Worldpop.

The land-consumption rate measures the physical expansion of the urban area (built-up area) relative to the population growth rate. Cities require an orderly expansion of the urban area to accommodate the internal population growth, migration and provision of the transportation and open-space services. However, the disproportionate physical growth of urban areas relative to population growth leads to inefficient and unsustainable land use that not only results in negative impacts on the environment but also negative consequences in social and economic terms [51]. Therefore, the measure of the indicator provides an important insight to the city planners about the urban expansion and population growth. The measure of the indicator also adds them in decision making for prioritising the areas for interventions to find a balance between growing population, built-up areas and provision of services (such as transportation and public open spaces).

The interpretation of the indicator, however, may give a dubious meaning. For instance, the ratio of 1 can be associated with both (1) urban compactness and ensuite of delivery of provisional services; and (2) congestions, ill management of urban expansion and deteriorating living standards [54]. The paper recommends further analysis of the indicator with additional sub-indicators for SDG 11.3.1 and validation of machine-learning results using ground data.

## 5. Conclusions

Global data and open geospatial tools can be used for climate risk assessment, land-degradation status and land-consumption indicators. The results aggregated at lower administrative levels can be helpful in decision making, preparing and planning the cities in the wake of climate change, food insecurity, population growth and increased urbanisation using simple analysis and through minimal use of local data. Global data and remote-sensing tools can play a vital role in undertaking such studies, especially in countries where local data are scarce and not readily available. Further, the present assessment made use of open satellite imagery (Sentinel, Landsat, NICFI planet) for image classification and fragmentation.

However, the accuracy of the result is challenging for validating the data. The results of this study can be a basis for policymakers in planning an inclusive climate adaptation measure and sustainable land-use frameworks and policies.

The present study selected the Analamanga region in Madagascar for climate risk assessment found eight Falkontany, viz. (1) Soavimasoandro, (2) Androhibe, (3) Ambodivoanjo Ambohijatovo Fara, (4) Analamahitsy Tanana, (5) Amorona, (6) Ambaravarankazo, (7) Alarobia Amboniloha and (8) Ambatobe, are at high risk from climate change. Similarly, in Kisumu county, Kenya, the measure of the land-degradation indicator showed that Migosi, Manyatta' B' and Kondele have higher degraded areas than other areas within the county. Therefore, these areas should be prioritised for land restoration and rehabilitation activities. Furthermore, Lena, Karankasso-Vigue and Koundougou departments in Houet province, Burkina Faso, have a higher land-consumption ratio. The findings demonstrate a higher need for intervention to find a balance between expanding the built-up area, accommodating the population and providing basic services (such as transportation and open spaces).

**Author Contributions:** Conceptualization, M.H. and S.A.; literature review, P.K. and S.A.; methodology and analysis, A.G., S.A. and P.K.; result and conclusion, S.A., P.K. and M.H.; orginal draft preparation, review and editing, P.K., A.G. and S.A.; supervision, M.H. All authors have read and agreed to the published version of the manuscript.

**Funding:** This research received no external funding.

**Acknowledgments:** The authors would like to acknowledge FAO Geospatial Unit and FAO Forestry team for their technical guidance and assistance with SEPAL; and UNU-EHS and MCII for their support with manuscript review.

**Conflicts of Interest:** The authors declare no conflict of interest.

## References

1. Gerland, P.; Raftery, A.E.; Ševčíková, H.; Li, N.; Gu, D.; Spoorenberg, T.; Alkema, L.; Fosdick, B.K.; Chunn, J.; Lalic, N.; et al. World Population Stabilization Unlikely This Century. *Science* **2014**, *346*, 234–237. [CrossRef] [PubMed]
2. Africapolis. Total Population. Available online: https://africapolis.org/en/data/?country=Africa&keyfigure=totalPop&type=growth&year=2015 (accessed on 18 April 2022).
3. World Bank. Population Growth (Annual%). Available online: https://data.worldbank.org/indicator/SP.POP.GROW?name_desc=true (accessed on 18 April 2022).
4. UNDESA. World Urbanization Prospects. In *Demographic Research*; United Nations, Department of Economic and Social Affairs, Population Division: New York, NY, USA, 2014; p. 126.

5. FAOSTAT. *Annual Population*; Food and Agriculture Organization of the United Nations: Rome, Italy, 2022.
6. Ray, D.K.; Ramankutty, N.; Mueller, N.D.; West, P.C.; Foley, J.A. Recent Patterns of Crop Yield Growth and Stagnation. *Nat. Commun.* **2012**, *3*, 1293. [CrossRef] [PubMed]
7. van Soesbergen, A.; Scott, E.; Arnell, A.; Sassen, M.; Darrah, S. *The Distribution of Threats from Future Agricultural Development to Biodiversity and Ecosystem Services in the Lake Victoria Basin: Implications for Policy*; UN Environment World Conservation Monitoring Centre (UNEP-WCMC): Cambridge, UK, 2018.
8. FAO. Regional Overview of Food Security and Nutrition in Africa 2016. In *The Challenges of Building Resilience to Shocks and Stresses*; FAO: Rome, Italy, 2017.
9. Lioubimtseva, E. *Africa and Global Climate Change: Impacts, Vulnerabilities and Adaptation Challenges, First*; Routledge: London, UK, 2014.
10. Wang, G.; Eltahir, E.A.B. Impact of $CO_2$ Concentration Changes on the Biosphere-Atmosphere System of West Africa. *Glob. Chang. Biol.* **2002**, *8*, 1169–1182. [CrossRef]
11. Eastwood, R.; Lipton, M.; Newell, A. Farm Size. In *Handbook of Agricultural Economics*; Elsevier: Amsterdam, The Netherlands, 2010.
12. Lindley, S.J.; Gill, S.E.; Cavan, G.; Yeshitela, K.; Nebebe, A.; Woldegerima, T.; Kibassa, D.; Shemdoe, R.; Renner, F.; Buchta, K.; et al. *Urban Vulnerability and Climate Change in Africa: Green Infrastructure for Climate Adaption in African Cities*; Springer: Berlin/Heidelberg, Germany, 2015. [CrossRef]
13. Matano, A.-S.; Kanangire, C.K.; Anyona, D.N.; Abuom, P.O.; Gelder, F.B.; Dida, G.O.; Owuor, P.O.; Ofulla, A.V.O. Effects of Land Use Change on Land Degradation Reflected by Soil Properties along Mara River, Kenya and Tanzania. *Open J. Soil Sci.* **2015**, *5*, 20–38. [CrossRef]
14. Olanipekun, I.O.; Olasehinde-Williams, G.O.; Alao, R.O. Agriculture and Environmental Degradation in Africa: The Role of Income. *Sci. Total Environ.* **2019**, *692*, 60–67. [CrossRef]
15. Lamourdia, T.; Tourino-Soto, I. Status and Trends in Land Degradation in Africa. In *Environmental Science and Engineering (Subseries: Environmental Science)*; Springer: Berlin/Heidelberg, Germany, 2007; pp. 39–53. [CrossRef]
16. FAO. FAO Strategic Framework 2022–2031. Available online: https://www.fao.org/strategic-framework/en (accessed on 9 April 2022).
17. Ingram, J.C.; Dawson, T.P. Climate Change Impacts and Vegetation Response on the Island of Madagascar. *Philos. Trans. R. Soc. A Math. Phys. Eng. Sci.* **2005**, *363*, 55–59. [CrossRef]
18. Weiskopf, S.; Cushing, J.; Morelli, T.L.; Myers, B. Climate Change Risks and Adaptation Options for Madagascar. *Ecol. Soc.* **2021**, *26*, 36. [CrossRef]
19. Fetraniaina, A.; Deliar, A.; Harto, A.B. Spatial Analysis of Urban Growth Based on City Center and Central Business District (a Case Study of Antananarivo, the Capital City of Madagascar). In *IOP Conference Series: Earth and Environmental Science*; IOP Publishing: Bristol, UK, 2019; Volume 389, p. 12010.
20. Andriamamonjisoa, S.N.; Hubert-Ferrari, A. Combining Geology, Geomorphology and Geotechnical Data for a Safer Urban Extension: Application to the Antananarivo Capital City (Madagascar). *J. Afr. Earth Sci.* **2019**, *151*, 417–437. [CrossRef]
21. Aubry, C.; Ramamonjisoa, J.; Dabat, M.; Rakotoarisoa, J.; Rakotondraibe, J.; Rabeharisoa, L. Urban Agriculture and Land Use in Cities: An Approach with the Multi-Functionality and Sustainability Concepts in the Case of Antananarivo (Madagascar). *Land Use Policy* **2012**, *29*, 429–439. [CrossRef]
22. Nematchoua, M.K.; Ricciardi, P.; Orosa, J.A.; Buratti, C. A Detailed Study of Climate Change and Some Vulnerabilities in Indian Ocean: A Case of Madagascar Island. *Sustain. Cities Soc.* **2018**, *41*, 886–898. [CrossRef]
23. Kuhl, L.; Van Maanen, K.; Scyphers, S. An Analysis of UNFCCC-Financed Coastal Adaptation Projects: Assessing Patterns of Project Design and Contributions to Adaptive Capacity. *World Dev.* **2020**, *127*, 104748. [CrossRef]
24. Sarkodie, S.A.; Ackom, E.; Bekun, F.V.; Owusu, P.A. Energy–Climate–Economy–Population Nexus: An Empirical Analysis in Kenya, Senegal, and Eswatini. *Sustainability* **2020**, *12*, 6202. [CrossRef]
25. Kipkemboi, B.; Lalit, K.; Richard, K. Climate Change and Variability in Kenya: A Review of Impacts on Agriculture and Food Security. *Environ. Dev. Sustain.* **2020**, *23*, 23–43. [CrossRef]
26. Karanja, I. An Enumeration and Mapping of Informal Settlements in Kisumu, Kenya, Implemented by Their Inhabitants. *Environ. Urban.* **2010**, *22*, 217–239. [CrossRef]
27. Goodess, C.; Berk, S.; Ratna, S.B.; Brousse, O.; Davies, M.; Heaviside, C.; Moore, G.; Pineo, H. Climate Change Projections for Sustainable and Healthy Cities. *Build. Cities* **2021**, *2*, 812. [CrossRef] [PubMed]
28. Koutsouris, A.J.; Destouni, G.; Jarsjö, J.; Lyon, S.W. Hydro-Climatic Trends and Water Resource Management Implications Based on Multi-Scale Data for the Lake Victoria Region, Kenya. *Environ. Res. Lett.* **2010**, *5*, 034005. [CrossRef]
29. Lee, J. Farmer Participation in a Climate-Smart Future: Evidence from the Kenya Agricultural Carbon Market Project. *Land Use Policy* **2017**, *68*, 72–79. [CrossRef]
30. Ajuang, C.O.; Abuom, P.O.; Bosire, E.K.; Dida, G.O.; Anyona, D.N. Determinants of Climate Change Awareness Level in Upper Nyakach Division, Kisumu County, Kenya. *Springerplus* **2016**, *5*, 1015. [CrossRef]
31. Ochieng, M.; Koske, J. The Level of Climate Change Awareness and Perception among Primary School Teachers in Kisumu Municipality, Kenya. *Int. J. Humanit. Soc. Sci.* **2013**, *3*, 174–179.
32. Abdallah, S.A.; Njoroge, T.M.; Jaoko, J.O. Assessment of Land Degradation by Rusle Model Using Remote Sensing and GIS: A Case Study of Kenya's Lake Victoria Basin. *Int. J. Agric. Environ. Biores.* **2018**, *3*, 26–49. [CrossRef]

33. Kizito, F.; Tamene, L.; Koech, N.; Pondi, B.; Ng'ang'a, K. Land Degradation Assessment Using Multiscale Hierarchical Approaches for Agroecosystem Restoration and Improved Food Security: The Case Study of Kenya and Burkina Fasox. *Int. Center Trop. Agric.* **2018**.
34. Basson, F.; Dayamba, S.; Korahire, J.; Dipama, J.; Zougmoré, F.; Neya, T. Institutional Barriers to Climate Change Adaptation in Burkina Faso: How Could We Go around Them? *J. Sustain. Dev.* **2020**, *13*, 67–78. [CrossRef]
35. Nana, T.J. Impact of Climate Change on Cereal Production in Burkina Faso. *J. Agric. Environ. Sci.* **2019**, *8*, 14–24. [CrossRef]
36. Knauer, K.; Gessner, U.; Fensholt, R.; Forkuor, G.; Kuenzer, C. Monitoring Agricultural Expansion in Burkina Faso over 14 Years with 30 m Resolution Time Series: The Role of Population Growth and Implications for the Environment. *Remote Sens.* **2017**, *9*, 132. [CrossRef]
37. Nati, B.; Delphine, A.; Alima, B.A.; Felix, K.K.; Nadine, F.; Ouedraogo, G.; Delphine, B.N.A.; Alima, B.A.; Felix, K.K.; Ouedraogo, F.N.G. Impact of Climate Variability on Water Requirements of Lowland Rice Farming in South Sudanian Climate Region. *J. Agric. Environ. Sci.* **2019**, *8*, 186–190. [CrossRef]
38. Ouedraogo, I.; Tigabu, M.; Savadogo, P.; Compaoré, H.; Odén, P.C.; Ouadba, J.M. Land Cover Change and Its Relation with Population Dynamics in Burkina Faso, West Africa. *Land Degrad. Dev.* **2010**, *21*, 453–462. [CrossRef]
39. Nebie, E.K.; West, C.T. Migration and Land-Use and Land-Cover Change in Burkina Faso: A Comparative Case Study. *J. Polit. Ecol.* **2019**, *26*, 614–632.
40. Fischer, G.; Nachtergaele, F.O.; van Velthuizen, H.T.; Chiozza, F.; Franceschini, G.; Henry, M.; Muchoney, D.; Tramberend, S. *Global Agro-Ecological Zone V4—Model Documentation*; Food Agriculture Organization: Rome, Italy, 2021. [CrossRef]
41. GAEZ. Global Agro-Ecological Zoning version 4 (GAEZ v4). Available online: https://gaez.fao.org/ (accessed on 10 April 2022).
42. WorldPop. World Population. Open Spatial Demographic Data and Research. Available online: https://www.worldpop.org/ (accessed on 18 April 2022).
43. UNISDR & World Bank. *Synthesis Report on Ten ASEAN Countries Disaster Risks Assessment*; UNISDR & World Bank: Washington, DC, USA, 2010.
44. UNSTAT. *SDG Indicators Metadata Repository*; United Nations Statistics Division Development Data and Outreach Branch; UNSTAT: New York, NY, USA, 2022.
45. Africover. Land Cover, Kenya (Africover, FAO). UN-SPIDER Knowledge Portal. Available online: https://un-spider.org/links-and-resources/data-sources/land-cover-kenya-africover-fao (accessed on 10 February 2022).
46. ISRIC. World Soil Information. SoilGrdis-Global Gridded Soil Information. Available online: https://www.isric.org/explore/soilgrids (accessed on 10 February 2022).
47. Sims, N.C.; Newnham, G.J.; England, J.R.; Guerschman, J.; Cox., S.J.D.; Roxburgh, S.H.; Viscarra Rossel, R.A.; Fritz, S.; Wheeler, I. *Good Practice Guidance. SDG Indicator 15.3.1, Proportion of Land That Is Degraded Over Total Land Area. Version 2.0*; United Nations Convention to Combat Desertification: Bonn, Germany; New York, NY, USA, 2021.
48. SEPAL. System for Earth Observations, Data Access, Processing and Analysis for Land Monitoring. Available online: https://sepal.io/ (accessed on 9 February 2022).
49. USAID. *Climate Risk Profile: East Africa*; World Bank: Washington, DC, USA, 2020.
50. USAID. *Climate Risk Profile: West Africa*; World Bank: Washington, DC, USA, 2018.
51. Ntihinyurwa, P.D.; De Vries, W.; Chigbu, U.; Dukwiyimpuhwe, P. The Positive Impacts of Farm Land Fragmentation in Rwanda. *Land Use Policy* **2019**, *81*, 565–581. [CrossRef]
52. UNEP. *The Economics of Land Degradation in Africa*; UNEP: Bonn, Germany, 2015. [CrossRef]
53. Yu, P.; Fennell, S.; Chen, Y.; Liu, H.; Xu, L.; Pan, J.; Bai, S.; Gu, S. Positive Impacts of Farmland Fragmentation on Agricultural Production Efficiency in Qilu Lake Watershed: Implications for Appropriate Scale Management. *Land Use Policy* **2022**, *117*, 106108. [CrossRef]
54. United Nations. *SDG Indicator Metadata*; United Nations: New York, NY, USA, 2021.